jraas

Journal of the Renin-Angiotensin-Aldosterone System
July-September 2017: 1–8

DOI: 10.1177/1470320317729281
journals.sagepub.com/home/jra
SAGE

Angiotensin-(1–7) attenuates atrial tachycardia-induced sympathetic nerve remodeling

Wenfeng Shangguan, Wen Shi, Guangping Li, Yuanyuan Wang, Jian Li and Xuewen Wang

Abstract

Introduction: The effect of Angiotensin-(1–7) (Ang-(1–7)) on atrial autonomic remodeling is still unknown. We hypothesized that Ang-(1–7) could inhibit sympathetic nerve remodeling in a canine model of chronic atrial tachycardia.

Materials and methods: Eighteen dogs were randomly assigned to sham group, pacing group and Ang-(1–7) group. Rapid atrial pacing was maintained for 14 days in the pacing and Ang-(1–7) groups. Ang-(1–7) was administered intravenously in the Ang-(1–7) group. The atrial effective refractory period and atrial fibrillation inducibility level were measured at baseline and under sympathetic nerve stimulation after 14 days of measurement. The atrial sympathetic nerves labeled with tyrosine hydroxylase were detected using immunohistochemistry and Western blotting, and tyrosine hydroxylase and nerve growth factor mRNA levels were measured by reverse transcription polymerase chain reaction.

Results: Pacing shortened the atrial effective refractory period and increased the atrial fibrillation inducibility level at baseline and under sympathetic nerve stimulation. Ang-(1–7) treatment attenuated the shortening of the atrial effective refractory period and the increase in the atrial fibrillation inducibility level. Immunohistochemistry and Western blotting showed sympathetic nerve hyperinnervation in the pacing group, while Ang-(1–7) attenuated sympathetic nerve proliferation. Ang-(1–7) alleviated the pacing-induced increases in tyrosine hydroxylase and nerve growth factor mRNA expression levels.

Conclusion: Ang-(1–7) can attenuate pacing-induced atrial sympathetic hyperinnervation.

Keywords

Angiotensin-(1–7), chronic atrial pacing, sympathetic nerve remodeling, atrial fibrillation, tyrosine hydroxylase

Date received: 31 December 2016; accepted: 31 July 2017

Introduction

Atrial fibrillation is the most common arrhythmia, and it is associated with a significant increase in morbidity and mortality.[1] Recent studies have demonstrated that atrial sympathetic nerve hyperinnervation may increase atrial fibrillation susceptibility.[2,3] Chronic atrial pacing could lead to sustained atrial fibrillation not only due to pacing-induced electrical and structural remodeling,[4–6] but also due to autonomic nerve remodeling.[7–10]

It has been demonstrated that the renin–angiotensin system (RAS) is involved in the initiation and maintenance of atrial fibrillation.[11] Angiotensin-(1–7) (Ang-(1–7)), as a novel member of the RAS, was confirmed to counterbalance the effects of Angiotensin II (Ang II).[12,13] Our previous studies indicated that Ang-(1–7) could prevent atrial electrical and structural remodeling in dogs with chronic atrial tachycardia.[14–16] The effects of Ang-(1–7) on atrial sympathetic nerve remodeling are still unknown. The purpose of this study was to investigate whether Ang-(1–7)

Tianjin Key Laboratory of Ionic-Molecular Function of Cardiovascular Disease, Department of Cardiology, Tianjin Institute of Cardiology, Second Hospital of Tianjin Medical University, China

Corresponding author:
Xuewen Wang, Tianjin Key Laboratory of Ionic-Molecular Function of Cardiovascular Disease, Department of Cardiology, Tianjin Institute of Cardiology, Second Hospital of Tianjin Medical University, Tianjin 300211, China.
Email: milanfans@163.com

had a protective effect on sympathetic nerve remodeling in chronic atrial tachycardia in dogs. We labeled the sympathetic nerve with tyrosine hydroxylase (TH) as previously reported.[10]

Materials and methods

Preparation of the canine model

All animal studies were approved by the experimental animal administration committee of Tianjin Medical University and Tianjin Municipal Commission for Experimental Animal Control. Eighteen mongrel dogs of either sex weighing between 12 and 14 kg were included in this study. All dogs were anesthetized with intravenous pentobarbital sodium (30 mg/kg) and ventilated with room air. Under sterile conditions, a modified unipolar J-shaped pacing lead (St. Jude Medical) was inserted through the right jugular vein and the distal end of the lead was positioned in the right atrium, as described in a previous study.[14] Initial atrial capture was verified using an external stimulator (ALC-V8, Shanghai Alcott Biotech CO. LTD, and China). The proximal end of the pacing lead was then connected to a programmable pacemaker (made in Shanghai Fudan University, China), which was inserted into a subcutaneous pocket in the neck. The dogs in the pacing and Ang-(1–7) groups were paced at 500 beats/min for a period of 14 days. The dogs in the sham group received a pacemaker implant but did not undergo pacing. During the pacing, Ang-(1–7) (6 μg/kg per h) (Bachem AG, Bubendorf, Switzerland) was given intravenously through a jugular vein catheter by an ALZET® osmotic pump (DURECT Corporation, Cupertino, CA, USA) continuously during pacing for 14 days. The surface electrocardiogram was verified to ensure continuous 1:1 atrial capture every other day. Direct systolic blood pressure was measured during anesthesia before and after 14 days' pacing by a multichannel physiological recorder (TOP 2001, Hongtong Inc., China).

Two weeks after the pacemaker implant, all dogs were intubated and mechanically ventilated with room air. Under sterile conditions, a median sternotomy was performed. Six pairs of electrodes (diameter: 1.5 mm; distance between poles: 1.5 mm) were stitched onto the left and right atrial epicardia. The corresponding sites were in the high left atrium, low left atrium, and left atrial appendage (HLA, LLA, and LAA, respectively), and in the same sites of the right atrium (HRA, LRA, and RAA, respectively).

Measurement of atrial effective refractory period and atrial fibrillation inducibility

The atrial effective refractory period (AERP) at each site was measured by programmed pacing from the multi-channel electrophysiology recorder (TOP 2001, Hongtong Inc., China). There were eight sequential stimuli (S1-S1, cycle length 250 ms) followed by one premature stimulus (S2) with a doubling pacing threshold. The S1–S2 interval progressively decreased by 10 ms and, subsequently, 2 ms near the refractory value to ensure accurate recording. AERPs were the longest coupling interval that failed to capture the atrium.

Atrial fibrillation was defined as P-wave disappearance and rapid atrial activation with irregular ventricular response and a duration of more than 1 s. Atrial fibrillation was induced at the above six atrial sites with a 5-s continuous burst stimulation, at 10 Hz with four thresholds and 0.5-ms duration pulses. The burst stimulation was repeated three times at each site and was recorded whenever atrial fibrillation was successfully induced. If the atrial fibrillation duration time was longer than 60 s, rapid atrial pacing or electrical conversion was used to reverse atrial fibrillation to sinus rhythm, since a prolonged period of atrial fibrillation may induce transient atrial remodeling, provoke longer episodes of atrial fibrillation and affect subsequent measurements.

After basic electrophysiological examination, the AERPs and atrial fibrillation inducibility level were measured under sympathetic nerve stimulation (SNS). The bilateral stellate ganglia were carefully isolated from the surrounding tissue. Two insulated bipolar electrodes were attached to the dorsal and ventral ansae of both stellate ganglia, which were then stimulated continuously with pulses of 5 V for a duration of 0.5 ms and a frequency of 10 Hz. The stimulus intensity was adjusted by the heart rate (HR), such that a HR increase of at least 30% was maintained when compared with the basal sinus rhythm rate throughout the measurement of AERPs and atrial fibrillation inducibility level.

Immunohistochemistry study

After completing the electrophysiological measurement, the left atrial (LA) and right atrial (RA) tissues were immediately cut off and washed with cold 0.9% sodium chloride, while part of the tissue was fixed in formaldehyde and used in immunohistochemistry studies. The remaining tissue was rapidly frozen in liquid nitrogen and stored separately at −80°C for molecular biological studies. Immunohistochemistry was performed to examine the density and distribution of the sympathetic nerves (TH-positive) in the atria. Five-micrometer (μm) sections were cut from paraffin blocks of the LA and RA free walls, which were then stained with TH to label the sympathetic nerves. In brief, six sections from the LA and the RA were used to analyze the sympathetic nerve density per canine. We determined the fibrosis area using a computer-assisted image analysis system (Image-Pro Plus 7.0, Media Cybernetics, USA). The labels of all slides were covered,

so that the investigator who counted the nerves was blinded to the dog identification at the time of the nerve count. Each slide was examined under a microscope, and six fields with the highest density of sympathetic nerves were selected by the investigator. The computer automatically detected the stained nerves in these fields by their brown color, and automatically calculated the area occupied by the nerves in the field. The nerve density was the nerve-positive stained area divided by the total area examined ($\mu m^2/mm^2$). The mean nerve density in these six selected fields was used to represent the nerve density of that slide.

Western blotting

LA and RA tissues from each group were prepared for Western blotting analysis. Protein was extracted with total protein extraction buffer. An equal amount of protein was loaded onto a 6% sodium dodecyl sulfate (SDS) denaturing polyacrylamide gel, separated by electrophoresis, transferred onto a polyvinylidene fluoride membrane (Merck Millipore, Billerica, MA, USA) and incubated with a specific primary antibody at 4°C overnight. The membranes were then washed and subsequently incubated with the secondary antibody conjugated to horseradish peroxidase. Proteins were visualized using enhanced chemiluminescence. Protein levels of TH were expressed as a ratio against the levels of glyceraldehyde-3-phosphate dehydrogenase (GAPDH). Antibody to TH (ab93291) was purchased from Abcam, Inc. (Cambridge, UK) and anti-rabbit IgG HRP conjugate (W4011) was purchased from Promega, Inc. (Madison, USA).

Reverse transcription polymerase chain reaction

One aliquot of each tissue sample was used to investigate the mRNA expression of TH and nerve growth factor (NGF). In brief, 100 mg of tissue was homogenized in 1 ml of TRIzol reagent (Invitrogen, USA). RNA was then extracted with chloroform, precipitated in isopropyl alcohol and subsequently dissolved in diethyl pyrocarbonate-treated water. The integrity of each sample was confirmed by analysis on a denaturing agarose gel. The concentration of total RNA was determined spectrophotometrically at a wavelength of 260 nm, and the RNA was stored at −80°C for later analysis. Specific oligonucleotide primer pairs used for the amplification of GAPDH, TH and NGF were designed according to the sequences obtained from GeneBank. The primers specific (forward/reverse) for each protein were: 5′-GGCGTGAACCATGAGAAG TAT-3/5′-GTGGAAGCAGGGATGATGTT-3′ (GAPDH), 5′-TTCCAGTGCACGC AGTACAT-3′/5′-CGAACTCCACT GTGAACCA-3′ (TH), and 5′-ACAGGACTCA CAG GAGCAAG-3′/5′-TCCAGTGCTTGGAGTCGAT-3′ (NGF). A 200 ng quantity of total RNA was converted to cDNA and subjected to reverse transcription polymerase chain reaction (RT-PCR) using a commercially available kit (TaKaRa, China). PCR was performed using the SYBR-Green PCR kit as described by the manufacturer (TransGen, Beijing, China). The PCR consisted of 44 cycles of 95°C for 30 s, 58°C for 30 s and 72°C for 45 s. The relative mRNA expression levels were normalized to the GAPDH gene according to the $2^{-\Delta\Delta Ct}$ method. All the PCR experiments were carried out in triplicate within each experiment, and the experiments were replicated at least three times.

Statistical analysis

All data were expressed as mean ± SD. Statistical comparisons among groups were performed with one-way analyses of variance (ANOVA). Subsequently, if significant effects were indicated by ANOVA, all significant data were analyzed with a *t*-test to evaluate the differences between individual mean values. The inducible rate of atrial fibrillation was analyzed with the exact probability test. A $p<0.05$ was considered statistically significant.

Results

HR and blood pressure

There was no significant difference in HR and systolic blood pressure between the three groups at baseline ($p>0.05$), and the HR and systolic blood pressure were not changed by atrial pacing in any of the groups ($p>0.05$; Table 1)

AERPs

Two weeks of chronic atrial pacing markedly shortened the AERPs in the pacing group compared with the sham group ($p<0.05$). The Ang-(1–7) treatment attenuated the pacing-induced AERPs. Shortening at the sites of the HRA, HLA and LLA reached statistical significance ($p<0.05$). SNS did not change the AERPs in the sham group ($p>0.05$), but significantly decreased the AERPs in the pacing group. Ang-(1–7) attenuated the pacing-induced AERPs. The AERP shortening under SNS, at the sites of the HRA, LRA, HLA and LLA, reached statistical significance, as compared with the pacing group ($p<0.05$; Table 2)

Inducible rate of atrial fibrillation

Compared with the sham group, the pacing group showed a significantly elevated atrial fibrillation inducibility level ($p<0.05$). The Ang-(1–7) treatment reduced the atrial fibrillation inducibility level compared with that in the pacing group ($p<0.05$), though it was still higher than that in the sham group ($p<0.05$). SNS increased the atrial

Table 1. Hemodynamic parameters before and after pacing in each group ($\bar{x} \pm s$).

	Heart rate (beats/min)			Systolic blood pressure (mmHg)		
Groups	Before pacing	After pacing	*p*	Before pacing	After pacing	*p*
Sham	165 ± 9	167 ± 12	0.763	134 ± 7	138 ± 6	0.855
Pacing	171 ± 11	174 ± 16	0.737	140 ± 10	138 ± 8	0.511
Ang-(1–7)	168 ± 10	166 ± 11	0.739	135 ± 6	136 ± 9	0.768
F	0.593	1.016		1.160	0.074	
p	0.565	0.386		0.340	0.929	

Table 2. AERPs among the three groups at baseline and under SNS.

AERP ($\bar{x} \pm s$, ms)	Group	HRA	LRA	RAA	HLA	LLA	LAA
Baseline	S	110.4 ± 8.8	105.6 ± 7.2	106 ± 8.3	101 ± 7.9	101.0 ± 5.5	102.0 ± 8.9
	P	90.4 ± 16.9*	87.1 ± 6.1*	88.7 ± 10.7*	85.1 ± 6.9*	81.3 ± 12.9*	85.6 ± 3.9*
	A	106.4 ± 8.8**	95.7 ± 6.8	94.7 ± 10.6	96.7 ± 8.7**	93.3 ± 7.3**	94.3 ± 9.6
SNS	S	103.6 ± 8.6	108.2 ± 8.2	101.8 ± 7.5	92.9 ± 9.7	102.0 ± 6.0	104.7 ± 7.9
	P	79.1 ± 14.5***	75.6 ± 8.6***	76.7 ± 12.6***	74.0 ± 10.4***	69.8 ± 10.2***	76.9 ± 9.8***
	A	95.2 ± 8.4****	88.7 ± 8.4****	86.7 ± 8.6	92.0 ± 12.6****	87.7 ± 8.2****	81.7 ± 9.6

AERPs in the pacing group were markedly shortened compared with those in the sham group at baseline (*p<0.05). Ang-(1–7) attenuated the pacing-induced AERP shortening at baseline (**p<0.05). AERPs in the pacing group significantly decreased compared with those in the sham group under SNS (***p<0.05). Compared with the pacing group, the Ang-(1–7) group showed attenuated pacing-induced AERP shortening under SNS (****p<0.05).
AERP: atrial effective refractory period; Ang-(1–7): Angiotensin-(1–7); SNS: sympathetic nerve stimulation; S: sham group; P: pacing group; A: Ang-(1–7) group; HRA: high right atrium; LRA: low right atrium; RAA: right atrial appendage; HLA: high left atrium; LLA: low left atrium; LAA: left atrial appendage.

Table 3. The atrial fibrillation inducibility level among the three groups ($\bar{x} \pm s$).

AF inducible rate (%)	Sham	Pacing	Ang-(1–7)
Baseline	9.6 ± 3.6	32.7 ± 7.6*	17.6 ± 4.5*,**
SNS	11.0 ± 4.5	40.8 ± 4.7*,***	20.5 ± 4.9*,**,****

The AF inducibility level was significantly elevated in the pacing group compared with that in the sham group (*p<0.05). The AF inducibility level in the Ang-(1–7) group was significantly decreased compared with that in the pacing group (**p<0.05). SNS significantly increased the AF inducibility level in the pacing group (***p<0.05). However, in the Ang-(1–7) group, SNS did not significantly increase the AF inducibility level as compared with that at baseline (****p>0.05).
AF: atrial fibrillation; Angiotensin-(1–7); SNS: sympathetic nerve stimulation.

fibrillation inducibility level only in the pacing group (p<0.05) and not in the Ang-(1–7) group (p>0.05; Table 3).

Sympathetic nerve density

Immunohistochemical staining showed that the density of TH-positive nerves in the RA and LA were all significantly increased in the pacing group compared with that in the sham group (LA: 3032±463 *vs*. 1613±725; RA: 3621±752 *vs*. 1180±441, p<0.05). Ang-(1–7) attenuated the atrial pacing-induced atrial sympathetic hyperinnervation (LA: 3032 ± 463 *vs*. 2156 ± 873; RA: 3621±752 *vs*. 2621±752, p<0.05; Table 4 and Figure 1).

The expression of TH protein

Western blotting showed that the level of TH protein was significantly increased in the pacing group compared with that in the sham group (p<0.05). In the sham group, the LA exhibited a higher level of TH protein, although this increase was not significant (p>0.05). In the pacing group, both the LA and RA TH protein levels were significantly increased (p<0.05), with the increase in the RA TH protein level being greater than the increase in the LA TH protein level, and the absolute increase in values reached statistical significance (RA *vs*. LA, p<0.05). Ang-(1–7) treatment reduced both the LA and RA TH protein levels compared with those in the pacing group (p<0.05), though they were still higher than those in the sham group (p<0.05; Figure 2).

mRNA levels of TH and NGF

RT-PCR showed that the TH and NGF mRNA levels were significantly increased in the pacing group (p<0.05), and that Ang-(1–7) treatment reduced the mRNA levels of TH

Table 4. Densities of TH-positive nerves in the atria of the three groups ($\bar{x} \pm s$).

Nerve density ($\mu m^2/mm^2$)	Sham		Pacing		Ang-(1–7)	
	LA	RA	LA	RA	LA	RA
TH	1613 ± 725	1180 ± 441	3032 ± 463*	3621 ± 752*	2156 ± 873*,**	2621 ± 752*,**

The densities of TH-positive nerves in the RA and LA were all significantly increased compared with those in the sham group (*p<0.05). Ang-(1–7) treatment reduced the TH-positive nerve densities compared with those of the pacing group (**p<0.05).
TH: tyrosine hydroxylase; Ang-(1–7): Angiotensin-(1–7); LA: left atrium; RA: right atrium.

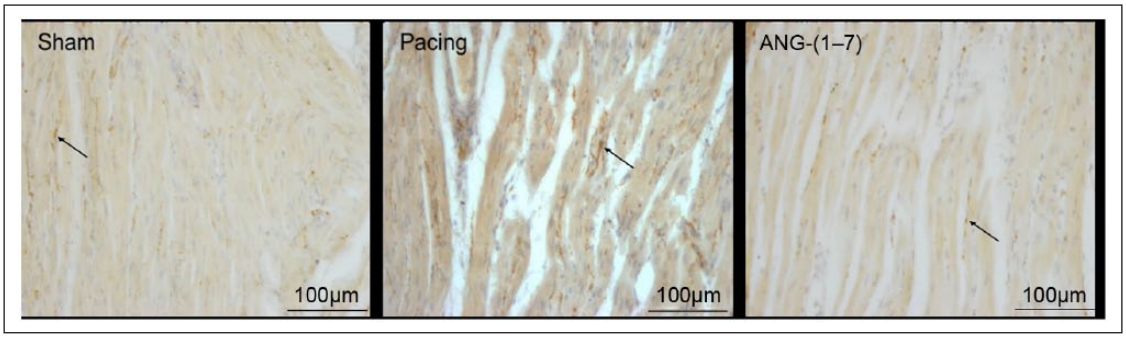

Figure 1. Typical examples of atrial tyrosine hydroxylase (TH)-positive nerve distribution (indicated by the arrows) in the three groups (200× magnification); The densities of the TH-positive nerves were significantly increased in the pacing group compared with those in the sham group; Ang-(1–7) attenuated the pacing-induced atrial sympathetic hyperinnervation.
Ang-(1–7): Angiotensin-(1–7).

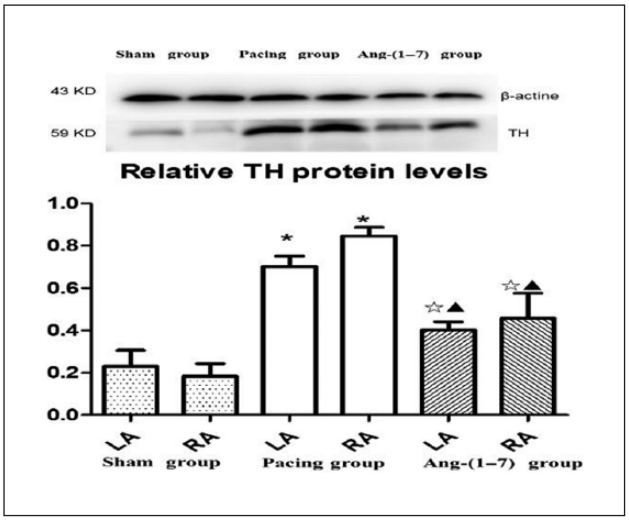

Figure 2. The relative TH protein levels among the three groups. Compared with the sham group, the TH protein level was significantly increased in the pacing group (✻p<0.05); Ang-(1–7) treatment reduced the TH protein levels compared with those in the pacing group (☆p<0.05), though they were still higher than those in the sham group (▲p<0.05).
Ang-(1–7): Angiotensin-(1–7); TH: tyrosine hydroxylase; LA: left atrium; RA: right atrium.

and NGF compared with those in the pacing group (p<0.05); however, the levels were still higher than those in the sham group (p<0.05; Figure 3).

Discussion

Main findings

The main findings of the present study were that two weeks of chronic atrial pacing induced atrial sympathetic hyperinnervation, and that Ang-(1–7) attenuated the pacing-induced atrial sympathetic hyperinnervation and had protective effects on atrial sympathetic nerve remodeling.

Effects of Ang-(1–7) on AERPs and atrial fibrillation

The electrophysiological changes in the chronic atrial tachycardia canine model observed in this study were similar to those reported in the previous studies. Ang-(1–7) modulates ionic channels[15] and prevents atrial tachycardia-induced ionic remodeling.[16] Ang-(1–7) has been shown to attenuate the rapid atrial pacing-induced shortening of AERPs and reduce the vulnerability of atrial fibrillation, thereby preventing atrial electrical remodeling.[17] Ang-(1–7) also prevented atrial electrical remodeling induced by atrial pacing through the Mas/PI3K/Akt/NO signaling pathway.[17]

Atrial fibrillation and atrial sympathetic nerve remodeling

Sympathetic nerve sprouting and proliferation may increase the atrial fibrillation inducibility level. In the present study,

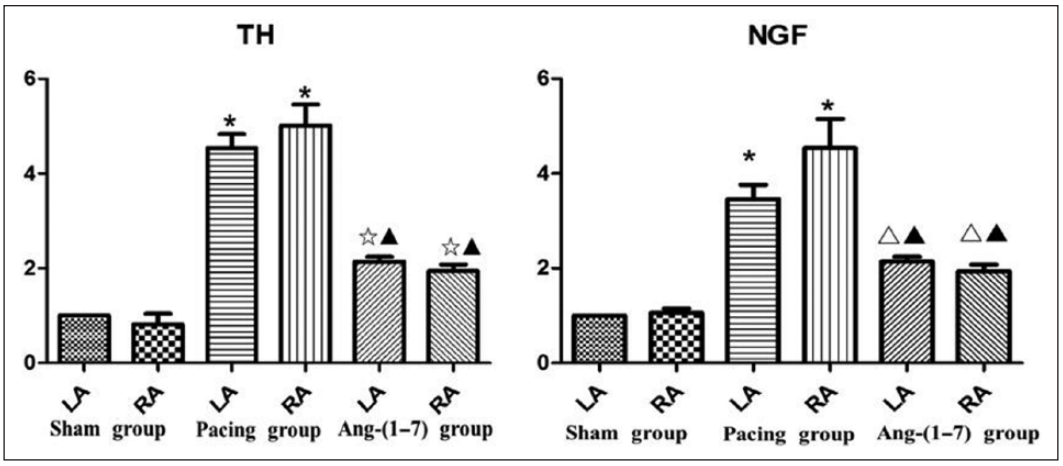

Figure 3. TH and NGF mRNA levels were significantly increased in the pacing group (*p<0.05), while Ang-(1–7) treatment reduced the mRNA levels of TH and NGF compared with those of the pacing group (☆p<0.05), though they were still higher than those in the sham group (▲p<0.05).
TH: tyrosine hydroxylase; NGF: nerve growth factor; LA: left atrium; RA: right atrium; Ang-(1–7): Angiotensin-(1–7).

sympathetic nerve sprouting and proliferation were found in the pacing group, and SNS decreased the AERPs and increased the atrial fibrillation inducibility level. Our findings are consistent with those of previous studies that demonstrated that cardiac sympathetic innervation plays a critical role in the dynamics of atrial fibrillation initiation and maintenance.[10] The catecholamines released by the proliferation sympathetic nerve endings were found to increase the heterogeneity of the AERPs and elevate the atrial fibrillation inducibility level.[18,19] Sympathetic hyperinnervation in the pulmonary vein provides a substrate for the trigger of rapid focal sources, thereby inducing some atrial fibrillation episodes.[20] Heterogeneous sympathetic innervation also facilitates sustained atrial fibrillation.[8] These findings indicate that sympathetic hyperinnervation may play an important role in the generation and maintenance of atrial fibrillation.

RAS-induced atrial sympathetic hyperinnervation

The RAS is widely distributed in the sympathetic nerve system and throughout the central nervous system, the peripheral nerve ganglia and even sympathetic nerve endings.[21–26] Activation of the RAS can directly affect the brain and sympathetic nerve ganglia, thereby increasing sympathetic outflow and causing excessive sympathoexcitation.[27–29] NGF is the main factor that stimulates the growth of sympathetic nerves,[30] and the RAS stimulates the synthesis of NGF,[31] thereby promoting the growth of sympathetic nerves and resulting in sympathetic nerve hyperinnervation. In the present study, significantly increased NGF mRNA expression levels were observed. During atrial fibrillation, the RAS has been shown to increase the mechanical stretch of atrial myocardial cells, resulting in the increased growth of sympathetic neurocytes.[32] Thus, the RAS plays an important role in the pathogenesis of sympathetic nerve sprouting and hyperinnervation.

Ang-(1–7) attenuates sympathetic nerve remodeling

Ang-(1–7) inhibits the RAS and attenuates sympathetic nerve remodeling. Gironacci et al.[33] demonstrated that Ang-(1–7) significantly decreased potassium-induced norepinephrine release in the hypothalamus by stimulating the Ang II receptor. Moreover, Ang-(1–7) was reported to inhibit the evoked release of norepinephrine from the hypothalamus.[34] Byku[35] also showed that Ang-(1–7) modulates sympathetic neurotransmitter overflow in a manner that might oppose the effects of Ang II on sympathetic neurotransmission. Ang II receptor blockers have been shown to inhibit the RAS and abolish the stretch-induced increase in NGF expression, thereby preventing stretch-induced neural growth.[36] Furthermore, Ang-(1–7) might abolish stretch-induced NGF expression and inhibit sympathetic nerve growth by counterbalancing the effects of Ang II. In the present study, we found that Ang-(1–7) inhibits the activity of the sympathetic nerves and attenuates both SNS-induced shortening of the AERPs and the increased atrial fibrillation inducibility level.

Our study showed, for the first time, that Ang-(1–7) could significantly attenuate atrial sympathetic hyperinnervation in a chronic atrial paced canine atrial fibrillation model. Electrical, structural and autonomic remodeling are the three main atrial remodeling mechanisms that act as the foundation of atrial fibrillation initiation and maintenance. Ang-(1–7) effectively suppresses all three of those mechanisms and has been speculated to act as an

effective agent in the treatment of atrial fibrillation; however, further clinical studies are necessary to verify this hypothesis.

Study limitations

Pentobarbital is known to prolong the AERP compared with the state of non-anesthesia, which may affect the atrial fibrillation inducibility level. We did not measure the levels of Ang-(1–7), which might have influenced the outcomes of this study. Unfortunately, we were unable to obtain specific canine NGF antibodies that could be used to measure the changes in NGF protein expression levels.

Conclusion

Ang-(1–7) significantly attenuated atrial sympathetic hyperinnervation in a chronic atrial pacing-induced canine atrial fibrillation model. These results might help to elucidate the relationship between the RAS and atrial fibrillation.

Acknowledgement

Wenfeng Shangguan and Wen Shi contributed equally to this work and should be considered co-first authors.

Declaration of conflicting interests

The authors declare that there is no conflict of interest.

Funding

This work was supported by the Specialized Research Fund for the Doctoral Program of Higher Education of China (grant no. 20121202120004) and the science and technology foundation of Tianjin sanitary bureau (grant no. 2015KZ105).

References

1. Kirchhof P, Bax J, Blomstrom-Lundquist C, et al. Early and comprehensive management of atrial fibrillation: Executive summary of the proceedings from the 2nd AFNET-EHRA consensus conference ‘research perspectives in AF’. *Eur Heart J* 2009; 30: 2969–2977c.
2. Zhao QY, Huang H, Zhang SD, et al. Atrial autonomic innervation remodelling and atrial fibrillation inducibility after epicardial ganglionic plexi ablation. *Europace* 2010; 12: 805–810.
3. Tan AY, Li H, Wachsmann-Hogiu S, Chen LS, et al. Autonomic innervation and segmental muscular disconnections at the human pulmonary vein-atrial junction: Implications for catheter ablation of atrial-pulmonary vein junction. *J Am Coll Cardiol* 2006; 48: 132–143.
4. Morillo CA, Klein GJ, Jones DL, et al. Chronic rapid atrial pacing. Structural, functional, and electrophysiological characteristics of a new model of sustained atrial fibrillation. *Circulation* 1995; 91: 1588–1595.
5. Gaspo R, Bosch RF, Talajic M, et al. Functional mechanisms underlying tachycardia-induced sustained atrial fibrillation in a chronic dog model. *Circulation* 1997; 96: 4027–4035.
6. Fareh S, Villemaire C and Nattel S. Importance of refractoriness heterogeneity in the enhanced vulnerability to atrial fibrillation induction caused by tachycardia-induced atrial electrical remodeling. *Circulation* 1998; 98: 2202–2209.
7. Liu L and Nattel S. Differing sympathetic and vagal effects on atrial fibrillation in dogs: Role of refractoriness heterogeneity. *Am J Physiol* 1997; 273: H805–H816.
8. Olgin JE, Sih HJ, Hanish S, et al. Heterogeneous atrial denervation creates substrate for sustained atrial fibrillation. *Circulation* 1998; 98: 2608–2614.
9. Schauerte P, Scherlag BJ, Patterson E, et al. Focal atrial fibrillation: experimental evidence for a pathophysiologic role of the autonomic nervous system. *J Cardiovasc Electrophysiol* 2001; 12: 592–599.
10. Chang CM, Wu TJ, Zhou S, et al. Nerve sprouting and sympathetic hyperinnervation in a canine model of atrial fibrillation produced by prolonged right atrial pacing. *Circulation* 2001; 103: 22–25.
11. Iravanian S and Dudley SC Jr. The renin–angiotensin–aldosterone system (RAAS) and cardiac arrhythmias. *Heart Rhythm* 2008; 5: S12–S17.
12. Santos RA, Castro CH, Gava E, et al. Impairment of in vitro and in vivo heart function in angiotensin-(1–7) receptor MAS knockout mice. *Hypertension* 2006; 47: 996–1002.
13. Grobe JL, Mecca AP, Lingis M, et al. Prevention of angiotensin II-induced cardiac remodeling by angiotensin-(1–7). *Am J Physiol Heart Circ Physiol* 2007; 292: H736–H742.
14. Liu E, Yang S, Xu Z, et al. Angiotensin-(1–7) prevents atrial fibrosis and atrial fibrillation in long-term atrial tachycardia dogs. *Regul Pept* 2010; 162: 73–78.
15. McKinney CA, Fattah C, Loughrey CM, et al. Angiotensin-(1–7) and angiotensin-(1–9): Function in cardiac and vascular remodelling. *Clin Sci (Lond)* 2014; 126: 815–827.
16. Liu E, Xu Z, Li J, et al. Enalapril, irbesartan, and angiotensin-(1–7) prevent atrial tachycardia-induced ionic remodeling. *Int J Cardiol* 2011; 146: 364–370.
17. Zhao J, Liu E, Li G, et al. Effects of the angiotensin-(1–7)/Mas/PI3K/Akt/nitric oxide axis and the possible role of atrial natriuretic peptide in an acute atrial tachycardia canine model. *J Renin Angiotensin Aldosterone Syst* 2015; 16: 1069–1077.
18. Miyauchi Y, Zhou S, Okuyama Y, et al. Altered atrial electrical restitution and heterogeneous sympathetic hyperinnervation in hearts with chronic left ventricular myocardial infarction: Implications for atrial fibrillation. *Circulation* 2003; 108: 360–366.
19. Taggart P, Sutton P, Lab M, et al. Interplay between adrenaline and interbeat interval on ventricular repolarisation in intact heart in vivo. *Cardiovasc Res* 1990; 24: 884–895.
20. Chen SA, Hsieh MH, Tai CT, et al. Initiation of atrial fibrillation by ectopic beats originating from the pulmonary veins: Electrophysiological characteristics, pharmacological responses, and effects of radiofrequency ablation. *Circulation* 1999; 100: 1879–1886.
21. Timmermans PB, Wong PC, Chiu AT, et al. Angiotensin II receptors and angiotensin II receptor antagonists. *Pharmacol Rev* 1993; 45: 205–251.

22. McKinley MJ, Albiston AL, Allen AM, et al. The brain renin–angiotensin system: Location and physiological roles. *Int J Biochem Cell Biol* 2003; 35: 901–918.
23. Cato MJ and Toney GM. Angiotensin II excites paraventricular nucleus neurons that innervate the rostral ventrolateral medulla: An in vitro patch-clamp study in brain slices. *J Neurophysiol* 2005; 93: 403–413.
24. Tang H, Pavel J, Saavedra JM, et al. Angiotensin II type 1 receptors may not influence response of spinal autonomic neurons to axonal damage. *Neurol Res* 2008; 30: 751–760.
25. Ahmad Z, Milligan CJ, Paton JF, et al. Angiotensin type 1 receptor immunoreactivity in the thoracic spinal cord. *Brain Res* 2003; 985: 21–31.
26. Patil J, Heiniger E, Schaffner T, et al. Angiotensinergic neurons in sympathetic coeliac ganglia innervating rat and human mesenteric resistance blood vessels. *Regul Pept* 2008; 147: 82–87.
27. Stadler T, Veltmar A, Qadri F, et al. Angiotensin II evokes noradrenaline release from the paraventricular nucleus in conscious rats. *Brain Res* 1992; 569: 117–122.
28. Tsuda K. Renin–angiotensin system and sympathetic neurotransmitter release in the central nervous system of hypertension. *Int J Hypertens* 2012; 2012: 474870.
29. Shinohara K, Kishi T, Hirooka Y, et al. Circulating angiotensin II deteriorates left ventricular function with sympathoexcitation via brain angiotensin II receptor. *Physiol Rep* 2015; 3.
30. Huang EJ and Reichardt LF. Neurotrophins: Roles in neuronal development and function. *Annu Rev Neurosci* 2001; 24: 677–736.
31. Jeffreson S, Rush R, Zettler C, et al. The influence of the renin angiotensin system on abnormal expression of nerve growth factor in the spontaneously hypertensive rat. *Clin Exp Pharmacol Physiol* 1995; 22: 478–480.
32. Rana OR, Schauerte P, Hommes D, et al. Mechanical stretch induces nerve sprouting in rat sympathetic neurocytes. *Auton Neurosci* 2010; 155: 25–32.
33. Gironacci MM, Valera MS, Yujnovsky I, et al. Angiotensin-(1–7) inhibitory mechanism of norepinephrine release in hypertensive rats. *Hypertension* 2004; 44: 783–787.
34. Gironacci MM, Yujnovsky I, Gorzalczany S, et al. Angiotensin-(1–7) inhibits the angiotensin II-enhanced norepinephrine release in coarcted hypertensive rats. *Regul Pept* 2004; 118: 45–49.
35. Byku M, Macarthur H and Westfall TC. Inhibitory effects of angiotensin-(1–7) on the nerve stimulation-induced release of norepinephrine and neuropeptide Y from the mesenteric arterial bed. *Am J Physiol Heart Circ Physiol* 2010; 298: H457–H465.
36. Rana OR, Schauerte P, Hommes D, et al. Mechanical stretch induces nerve sprouting in rat sympathetic neurocytes. *Auton Neurosci* 2010; 155: 25–32.